Journal of Solid State Chemistry 183 (2010) 620–623

Contents lists available at ScienceDirect

Journal of Solid State Chemistry

journal homepage: www.elsevier.com/locate/jssc

Luminescence enhancement of Eu^{2+}, Ce^{3+} co-doped $Ba_3Si_5O_{13-\delta}N_\delta$ phosphors

Ruili Zhang [a,b], Tomonori Maeda [b], Ryosuke Maruta [b], Sho Kusaka [b], Bingjun Ding [a], Kei-ichiro Murai [b], Toshihiro Moriga [b,*]

[a] State Key Laboratory for Mechanical Behavior of Materials, School of Materials Science and Engineering, Xi'an Jiaotong University, Shaanxi 710049, China
[b] Department of Chemical Science and Technology, Graduate School of Advanced Technology and Science, The University of Tokushima, 2-1 Minami-Josanjima, Tokushima 770-8506, Japan

ARTICLE INFO

Article history:
Received 1 September 2009
Received in revised form
2 December 2009
Accepted 14 December 2009
Available online 23 December 2009

Keywords:
$Ba_3Si_5O_{13-\delta}N_\delta$ $Eu^{2+}Ce^{3+}$
Co-doping
Phosphor
White LEDs

ABSTRACT

Host lattice $Ba_3Si_5O_{13-\delta}N_\delta$ oxonitridosilicates have been synthesized by the traditional solid state reaction method. The lattice structure is based on layers of vertex-linked SiO_4 tetrahedrons and Ba^{2+} ions, where each Ba^{2+} ion is coordinated by eight oxygen atoms forming distorted square antiprisms. Under an excitation wavelength of 365 nm, $Ba_3Si_5O_{13-\delta}N_\delta$:$Eu^{2+}$ and $Ba_3Si_5O_{13-\delta}N_\delta$:$Eu^{2+}$,$Ce^{3+}$ show broad emission bands from about 400–620 nm, with maxima at about 480 nm and half-peak width of around 130 nm. The emission intensity is strongly enhanced by co-doping Ce^{3+} ions into the $Ba_3Si_5O_{13-\delta}N_\delta$:$Eu^{2+}$ phosphor, which could be explained by energy transfer. The excitation band from the near UV to the blue light region confirms the possibility that $Ba_3Si_5O_{13-\delta}N_\delta$:$Eu^{2+}$, Ce^{3+} could be used as a phosphor for white LEDs.

1. Introduction

Since the invention of blue-light-emitting diodes (b-LEDs) based on (In,Ga)N chips by Nichia corporation [1], the concept of white-light-emitting diodes (w-LEDs) composed of blue-emitting LEDs and phosphor materials has also been raised [2,3]. The w-LEDs are expected to be a next-generation illumination light source offering high light efficiency, low energy consumption, and long service life. Currently available commercial white LEDs are composed of blue-emitting (In,Ga)N LEDs with yellow phosphors, typically Ce^{3+} doped yttrium aluminum garnet (YAG:Ce^{3+}) [4]. This white light, produced by mixing blue and yellow light, offers high luminescence efficiency but a poor color rendering index (CRI) [5]. To meet the optimum requirements of w-LEDs, phosphor materials with improved properties are in great demand.

As host lattices, the *M*–Si/Al–O–N or *M*–Si/Al–N (*M*=Mg, Ca, Sr or Ba) series have attracted great interest owing to their outstanding thermal, chemical and mechanical stability and structural diversity. Examples include red phosphors for $M_2Si_5N_8$:Eu^{2+} or $MSiN_2$:Eu^{2+} (*M*=Ca, Sr or Ba), $MgSiN_2$:Mn^{2+} [6–8], orange to yellow color-tunable phosphors for $(Sr_{(1-u)}Ba_u)Si_2O_2N_2$:$Eu^{2+}$ [9]. $M_2Si_5N_8$:Mn^{2+} [10] (*M*=Ca, Sr or Ba), yellow phosphors for Ba_3SiO_5:Eu^{2+} [11], or green phosphors for Ba_2SiO_4:Eu^{2+} [12], blue to yellow color-tunable phosphor Li_2SrSiO_4:Eu^{2+},Ce^{3+} [13].

As with the host lattice, activators also play an important role in the luminescent properties of phosphor materials. Since the *f–d* electron transitions for Eu^{2+} and Ce^{3+} ions and the *d–d* electron transitions for Mn^{2+} ions, Eu^{2+},Ce^{3+} and Mn^{2+} ions are often used as the activators, either separately or co-doped for LED phosphor materials [6,13]. Co-doping of the activators is an efficient method to obtain down-conversion phosphors, in which energy transfer is likely to occur [14,15]. It is reported that the emission is strongly enhanced in $LiSrSiO_4$:Eu^{2+},Ce^{3+} phosphors, with the Ce^{3+} acting as a sensitizer, while Eu^{2+} acts as an activator [13]. This combination is possibly applicable for other host lattice structures.

The $Ba_3Si_5O_{13}$ lattice structure has been reported in the 1980s [16], however, using this structure as the host lattice for phosphors, has not been reported to our knowledge. In our present work, the host lattice $Ba_3Si_5O_{13-\delta}N_\delta$ with co-doped Eu^{2+} and Ce^{3+} ions was successfully synthesized using traditional solid state reactions. The crystal structure and the photoluminescence properties of these samples are discussed.

2. Experimental section

2.1. Preparation

A series of $Ba_{3(1-x-y)}Si_5O_{13-\delta}N_\delta$:$xEu^{2+}$,$yCe^{3+}$ (*x*: Eu^{2+} content as a dopant, $0 \le x \le 2\%$; *y*: Ce^{3+} content as a dopant, $0 \le y \le 2\%$) were weighed out by molar ratio with the starting materials $BaCO_3$(Kanto Chemical, >99.95%), Si_3N_4 (Aldrich), Eu_2O_3 (Kanto

* Corresponding author.
E-mail address: moriga@chem.tokushima-u.ac.jp (T. Moriga).

0022-4596/$ - see front matter © 2009 Elsevier Inc. All rights reserved.
doi:10.1016/j.jssc.2009.12.011

Chemical, >99.95%) and CeO_2 (Kanto Chemical, >99.99%). and subsequently homogeneously mixed with an agate mortar and a pestle. The ratio of barium and the dopants to silicon was fixed to be 3:5. After mixing, the powder mixtures were fired in alumina crucibles at 1000 °C for 5 h under a NH_3 flow at a rate of 50 cm^3/min in a horizontal tube furnace. After firing, the samples were cooled to room temperature in the furnace.

2.2. Characterization

Phase identification: The obtained samples were identified by X-ray powder diffraction (XRD, RINT2500, Rigaku) with Cu $K\alpha$ radiation operating at 30 kV and 100 mA, and the data were collected with a step size of 0.02° and scanning speed of 4°/min.

The oxygen and nitrogen (O/N) contents of the powders were obtained by a gas extraction method using a Horiba EMGA-820 analyzer. Roughly 20 mg of a sample powder was placed in a graphite crucible with Ni and Sn pellets as flux, which was heated up above 3000 °C within a few seconds. Oxygen in the sample was converted to carbon monoxide while nitrogen evolved in its molecular form. The amount of both gases was determined using infrared and thermal conductivity detectors. Y_2O_3 and α-Si_3N_4 were used as references for oxygen and nitrogen contents.

Optical measurements: The diffuse reflectance spectra of samples were measured at room temperature by a JASCO V550 spectrophotometer (wavelength accuracy < 1 nm) equipped with a Xe flash lamp and an integrating sphere. The reflection spectra were calibrated with the reflection of a PTFE (poly-tetrafluoroethylene) compact in the wavelength region of 200–700 nm. The emission and excitation spectra were measured using fluorescent spectrophotometers (Hitachi F-7000) with a Xe-lamp as excitation source. The excitation and emission slits were set at 10 nm. All the spectra were measured with a scan speed of 100 nm/min.

3. Results and discussion

3.1. Phase identification

Fig. 1 shows the XRD patterns for $Ba_{3(1-x-y)}Si_5O_{13-\delta}N_\delta$:$xEu^{2+}$,$yCe^{3+}$ ($0 \le x \le 2\%, 0 \le y \le 2\%$). All the XRD patterns agree well with that for $Ba_3Si_5O_{13}$ (JCPDS# 26-0179), with a monoclinic unit cell and $p2_1/c$ space group. The structure of $Ba_3Si_5O_{13}$ is depicted as Fig. 2. From the *b* direction (Fig. 2a), the structure of $Ba_3Si_5O_{13}$ is based on layers of vertex-linked [SiO_4] tetrahedrons and Ba^{2+} ions; while from the *c* direction (Fig. 2b), six SiO_4 tetrahedrons form a ring of Si_6O_6, where each Ba^{2+} ion is coordinated to eight oxygen atoms forming [BaO_8] distorted square antiprisms [16]. In the $Ba_3Si_5O_{13-\delta}N_\delta$ structure, Eu^{2+} and Ce^{3+} would occupy the position for Ba^{2+} ions.

With doping of Eu^{2+} and Ce^{3+} ions, there is no apparent shift in the peak position compared with the $Ba_3Si_5O_{13-\delta}N_\delta$ host lattice, indicating that neither significant host lattice distortion, nor expansion/reduction occurred. According to the results of O/N content analysis, about 2.6% of oxygen atoms in $Ba_3Si_5O_{13}$ lattice are substituted by nitrogen atoms. The chemical formulae of the selected samples determined by the analysis are listed in Table 1. The formulae were calculated so that barium and silicon contents did not vary after firing. Anion nonstoichiometry in the samples was very small and the nitrogen ratio increased with an increase in Ce^{3+} content. The total nitrogen content seemed very small even though the starting materials are fired under the pure ammonia flow; however, this ammonia atmosphere is very important to form the $Ba_3Si_5O_{13}$ host lattice structure, since the

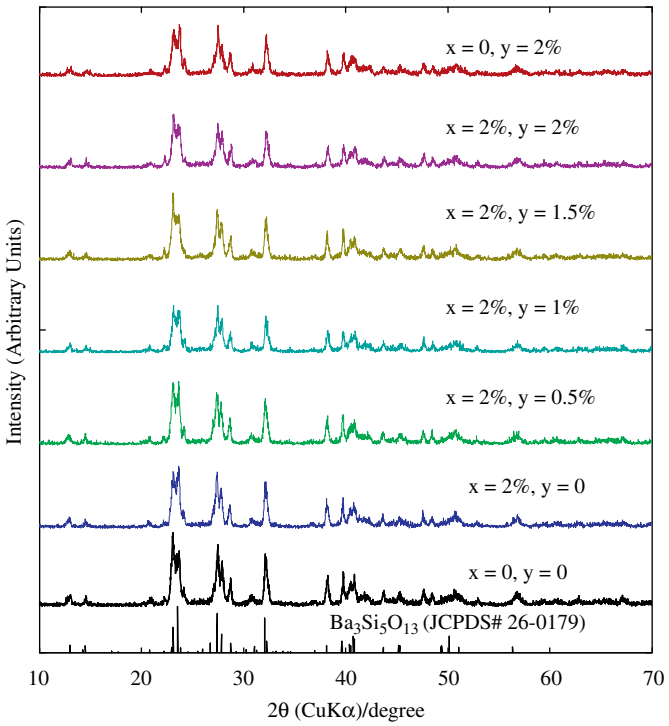

Fig. 1. XRD pattern for $Ba_{3(1-x-y)}Si_5O_{13-\delta}N_\delta$:$xEu^{2+}$,$yCe^{3+}$ ($0 \le x \le 2\%, 0 \le y \le 2\%$) prepared under NH_3 atmosphere.

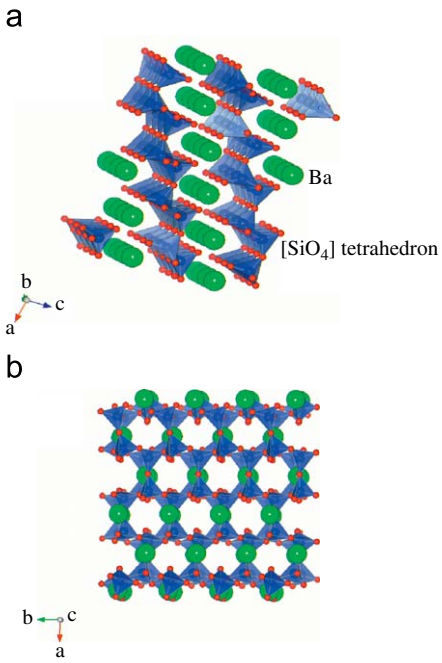

Fig. 2. Crystal structure of $Ba_3Si_5O_{13}$ (drawn with VENUS developed by Dilanian and Izumi).

Table 1
N/O contents and δ values of $Ba_3Si_5O_{13-\delta}N_\delta$.

Eu (%)	Ce (%)	N/O (%)	$Ba_3Si_5O_{13-\delta}N_\delta$
0	0	2.46	$Ba_3Si_5O_{12.68}N_{0.32}$
2	0	2.37	$Ba_3Si_5O_{12.69}N_{0.31}$
2	1	2.82	$Ba_3Si_5O_{12.63}N_{0.37}$
2	1.5	2.95	$Ba_3Si_5O_{12.62}N_{0.38}$

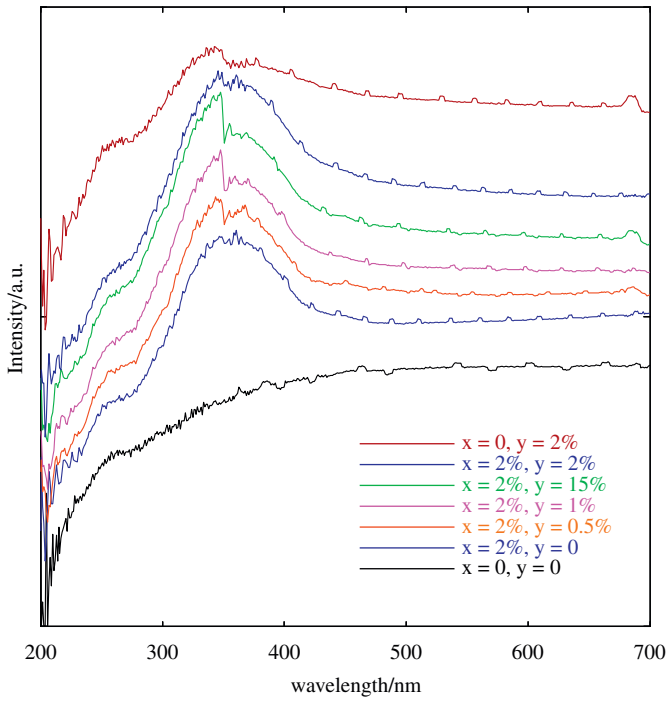

Fig. 3. Diffuse reflectance spectra for $Ba_{3(1-x-y)}Si_5O_{13-\delta}N_\delta$:$xEu^{2+}$,$yCe^{3+}$ ($0 \le x \le 2\%, 0 \le y \le 2\%$) prepared under NH_3 atmosphere.

main products formed under a nitrogen flow are $BaSi_2O_2N_2$ and $Ba_3Si_6O_{12}N_2$ as reported in earlier work [17].

3.2. *Diffuse reflectance spectra for $Ba_{3(1-x-y)}Si_5O_{13-\delta}N_\delta$:$Eu^{2+}$,$Ce^{3+}$*

Fig. 3 shows the diffuse reflectance spectra of $Ba_{3(1-x-y)}Si_5O_{13-\delta}N_\delta$:$xEu^{2+}$,$yCe^{3+}$ ($0 \le x \le 2\%, 0 \le y \le 2\%$). All samples were gray–white daylight color and showed an absorption band around 270 nm (4.6 ev) in the UV range, which is due to the valence-to-conduction band transition of $Ba_3Si_5O_{13-\delta}N_\delta$ host lattice (x(Eu^{2+} content)=0, y(Ce^{3+} content)=0). For a given value of x=2%, irrespective of the presence of Ce^{3+} ions, the absorption band appeared in the UV to blue light range (350–460 nm). For x=0, y=2%, this absorption band from 350 to 460 nm almost disappeared. We can conclude that the absorption band from 350 to 460 nm was mainly caused by the 4*f*-5*d* transition of Eu^{2+} ions in the $Ba_3Si_5O_{13-\delta}N_\delta$ structure, while the *f*–*d* transition hardly occurred when only Ce^{3+} ions existed. However, with increasing Ce^{3+} concentration from 0.5% to 1.5%, the absorption band is enhanced, showing the enhancing effect of Ce^{3+} ions to the Eu^{2+} ions. On the other hand, when Ce^{3+} concentration reached to 2%, the absorption band decreased slightly, which may be explained by the solubility of Ce^{3+} ions in the $Ba_3Si_5O_{13-\delta}N_\delta$ host lattice.

3.3. *Emission and excitation spectra for $Ba_{3(1-x-y)}Si_5O_{13-\delta}N_\delta$:$Eu^{2+}$,$Ce^{3+}$*

The emission spectra of $Ba_{3(1-x-y)}Si_5O_{13-\delta}N_\delta$:$xEu^{2+}$,$yCe^{3+}$ ($0 \le x \le 2\%, 0 \le y \le 2\%$) and YAG: Ce^{3+} (donated by Nichia Chemical Industries, and used as reference) is shown in Fig. 4. Under an excitation wavelength of 365 nm (Fig. 4a), corresponding to the diffuse spectra, the Eu^{2+}-free sample, $Ba_3Si_5O_{13-\delta}N_\delta$:$Ce^{3+}$ barely emitted light. The spectra for the other samples showed strong and broad emission bands from about 400–620 nm, covering the blue to orange region, with the maxima at around 460–480 nm, appearing as a bluish-white color, and width at half-peak height of around 130 nm. The emission intensity rapidly degraded with an increase in

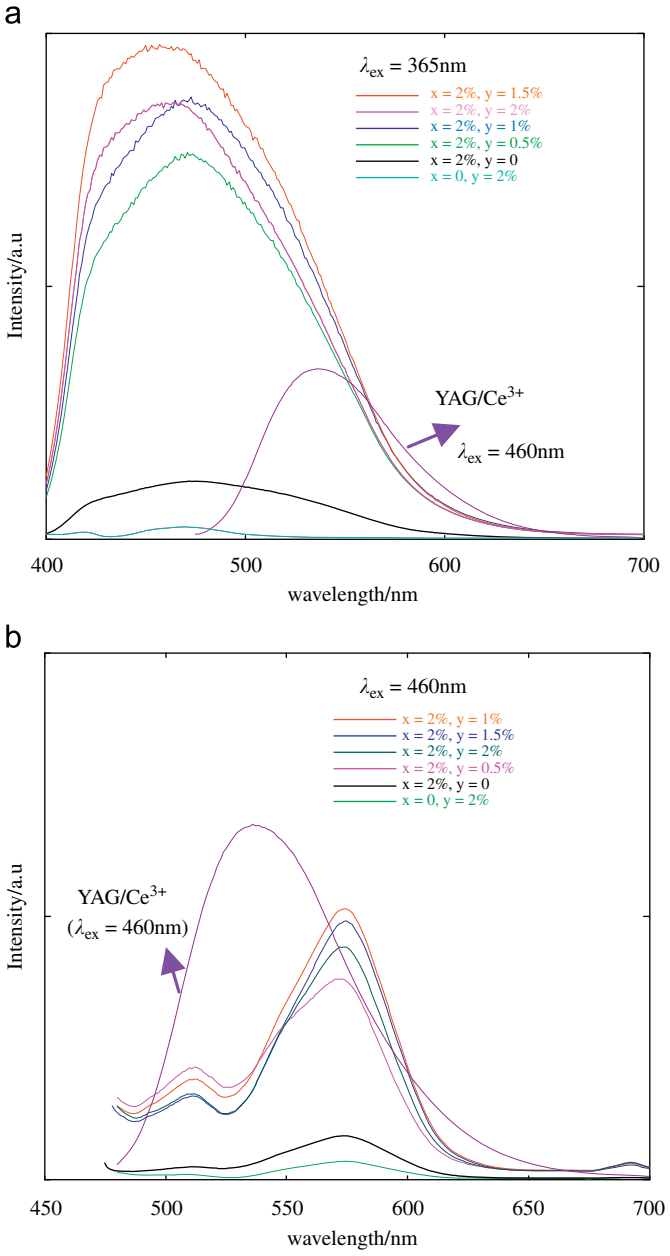

Fig. 4. Emission spectra for $Ba_{3(1-x-y)}Si_5O_{13-\delta}N_\delta$:$xEu^{2+}$,$yCe^{3+}$ ($0 \le x \le 2\%, 0 \le y \le 2\%$) (a) under the excitation wavelength of 365 nm. (b) under the excitation wavelength of 460 nm.

temperature, and reached to ca. 50% at 100 °C, compared with that at room temperature.

The broad emission appeared to be asymmetric, indicating that there are possibly two or more emission peaks. It can be presumed that Eu^{2+} and Ce^{3+} ions occupy different types of sites in the $Ba_3Si_5O_{13-\delta}N_\delta$ host lattice, forming corresponding emission centers. Another possible reason for broad band can be explained by the crystal field splitting effect. As mentioned above, in $Ba_3Si_5O_{13}$ compounds, each Ba^{2+} is coordinated by eight oxygen atoms and forms a [BaO_8] distorted square antiprism,. For the substitution of Ba^{2+} ions, Eu^{2+} and Ce^{3+} ions would also form [EuO_8] and [CeO_8] distorted square antiprisms. Like E_g and T_{2g} splitting in octahedral or tetrahedral coordination, the *d*-orbital for Eu^{2+} or Ce^{3+} could also be split in distorted square antiprisms. In the emission process, different energy releases would cause the peak overlap, forming a broad peak. Of course, for the nitrogen

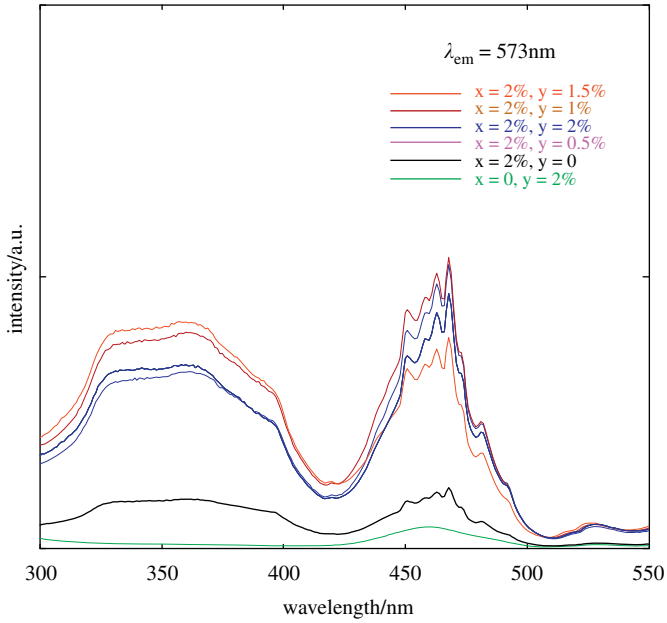

Fig. 5. Excitation spectra for $Ba_{3(1-x-y)}Si_5O_{13-\delta}N_\delta$:$xEu^{2+}$,$yCe^{3+}$ ($0 \le x \le 2\%$, $0 \le y \le 2\%$) under the emission wavelength of 573 nm.

atoms in the phosphors, the energy splitting would also be more complicated than that in $Ba_3Si_5O_{13}$ oxides, which could also be a reason for the broad emission bands as shown in Fig. 4(a).

While under the excitation wavelength of 460 nm (Fig. 4b), different emission bands, one weak peak at 512 nm and one strong peak at 573 nm appeared, confirming the existence of two possible emission centers in $Ba_3Si_5O_{13-\delta}N_\delta$ host lattice. The latter orange–yellow emitting property under blue light excitation is very significant. Although the emission intensity was slightly lower than that of YAG: Ce^{3+}, the emission wavelength was longer than that for the YAG: Ce^{3+} phosphor, making it a possible complement to the YAG: Ce^{3+} phosphor in blue-LEDs+YAG:Ce^{3+} white light systems to improve the luminescence properties.

However, in both situations, the emission intensity was strongly enhanced by increasing the Ce^{3+} concentration with a maximum at about 1.5%. This is about three times that of the YAG:Ce^{3+} phosphor under 365 nm excitation. This can be attributed to the typical energy transfer between two transition metals or rare-earth ions that is Eu^{2+} and Ce^{3+} ions in this case. When only Ce^{3+} ions exist, the Ce^{3+} ions hardly emit light; when Eu^{2+} and Ce^{3+} ions both exist, the emission intensity is much stronger than that when only Eu^{2+} ions exist. Hence, in the emitting process, Ce^{3+} ions probably act as a sensitizer, while the Eu^{2+} ions act as an activator, such that the effective emitting energy transfer from Ce^{3+} ions to Eu^{2+} ions, causes the emitting intensity to be enhanced [13].

Fig. 5 shows the excitation spectra of $Ba_{3(1-x-y)}Si_5O_{13-\delta}N_\delta$:$xEu^{2+}$,$yCe^{3+}$($0 \le x \le 2\%$,$0 \le y \le 2\%$) under an emission wavelength of 573 nm at room temperature. All the samples showed very similar band shape, although the excitation intensity was different with different Ce^{3+} concentration. The spectra showed a broad excitation band from 325 to 395 nm and a sharp, strong excitation band around 460 nm. This UV to visible light region excitation was merely reported for phosphors, allowing them to be the potential down-conversation phosphors excited both by UV LEDs or blue LEDs.

4. Conclusions

$Ba_3Si_5O_{13-\delta}N_\delta$ host lattice for phosphors have been synthesized by the traditional solid state reaction method. $Ba_3Si_5O_{13-\delta}N_\delta$: Eu^{2+}, Ce^{3+} phosphors show a broad emission band from 400 to 620 nm under 365 nm excitation and orange–yellow emission at 573 nm under 460 nm excitation. The excitation band of the phosphors is from about 300–500 nm, covering the UV to blue light region. The emission intensity is strongly enhanced by co-doping Ce^{3+} ions with the maximum concentration at 1.5%.

Acknowledgments

Authors thank Prof. James B. Metson of Department of Chemistry, University of Auckland for paper editing of this manuscript. This work was partly supported by a Grant-in-Aid (Approved no. 19018020) for Scientific Research on Priority Area entitled "Panoscopic Assembling and Highly Ordered Functions for Rare Earth Materials" from the Ministry of Educations, Culture, Sports, Science and Technology of Japan.

References

[1] S. Nakamura, T. Mukai, M. Senoh, Appl. Phys. Lett. 64 (1994) 1687–1689.
[2] W.M. Yen, S. Shionoya, H. Yamamoto (Eds.), Phosphor Handbook, second ed, CRC Press, Boca Raton, FL, 2006, pp. 533–543.
[3] R. Mueller-Mach, G.O. Mueller, Proc. SPIE 3938 (2000) 30–41.
[4] K. Bando, K. Sakano, Y. Noguchi, Y. Shimizu, J. Light Visual Environ. 22 (1998) 2–5.
[5] X.Q. Piao, K. Machida, T. Horikawa, H. Hanzawa, Chem. Mater. 19 (2007) 4592–4599.
[6] X.Q. Piao, T. Horikawa, H. Hanzawa, K. Machida, J. Electrochem. Soc. 153 (12) (2006) H232–H235.
[7] C.J. Duan, X.J. Wang, W.M. Otten, A.C.A. Delsing, J.T. Zhao, H.T. Hintzen, Chem. Mater. 20 (2008) 1597–1605.
[8] C.J. Duan, A.C.A. Delsing, H.T. Hintzen, J. Lumin. 129 (2009) 645–649.
[9] B.G. Yun, Y. Miyamoto, H. Yamamoto, J. Electrochem. Soc. 154 (10) (2007) J320–J325.
[10] C.J. Duan, W.M. Otten, A.C.A. Delsing, H.T. Hintzen, J. Solid State Chem. 181 (2008) 751–757.
[11] J.K. Park, M.A. Lim, K.J. Choi, C.H. Kim, J. Mater. Sci. 40 (2005) 2069–2071.
[12] M.A. Lim, J.K. Park, C.H. Kim, H.D. Park, J. Mater. Sci. 22 (2003) 1351–1353.
[13] X.L. Zhang, H. He, Z.S. Li, T. Yu, Z.G. Zou, J. Lumin. 128 (2008) 1876–1879.
[14] C.F. Zhu, Y.X. Yang, X.L. Liang, S.L. Yuan, G.R. Chen, J. Lumin. (2007) 707–710.
[15] S. Ye, Z.S. Liu, X.T. Wang, J.G. Wang, L.X. Wang, X.P. Jing, J. Lumin. 1296 (2009) 50–54.
[16] K.F. Hesse, F. Liebau, Zeitschrift für Kristallographie 153 (1980) 3–17.
[17] R.L. Zhang, M. Numada, T. Maeda. Y. Akazawa. K.I. Murai, T. Moriga, Int. J. Mod. Phys. B, in press.